THE ASTROPHYSICAL JOURNAL, **298**:808–817, 1985 November 15

MOLECULES AND DUST TOWARD CASSIOPEIA A

T. H. TROLAND
Physics and Astronomy Department, University of Kentucky

RICHARD M. CRUTCHER
Astronomy Department, University of Illinois

AND

CARL HEILES
Astronomy Department, University of California, Berkeley
Received 1984 June 25; accepted 1985 March 11

ABSTRACT

We report on ^{12}CO (J = 1–0 and J = 2–1) and ^{13}CO (J = 1–0) observations across the face of Cas A and at some adjacent positions. All the CO-emitting gas lies in front of the continuum source. Although little spatial structure exists in the Local Arm velocity components, structure on a scale of 1′–2′ (1–2 pc) is found within the Perseus Arm components. The CO structure correlates very well with the distributions of H_2CO and OH absorption toward Cas A as revealed by higher resolution synthesis maps. At velocities where a comparison is possible, the CO gas distribution bears some likeness to that of H I. We argue that the CO must be clumped on a scale smaller than the 1.′1 beamwidth of most of our observations and that the gas lies predominantly in dark rather than diffuse clouds. We estimate gas densities in the CO-emitting regions to be mostly in the range of one to a few times 10^3 cm^{-3}. These values are several times smaller than the densities derived by other authors from H_2CO data. Optical extinctions, estimated from the present CO study and from H I synthesis data of other authors, probably lie in the range 4–8 mag when averaged over an angular scale of $\sim 1'$. Actual extinctions along selected lines of sight must be higher owing to the small-scale clumping of the molecular gas. One such clump, seen in the H_2CO and OH synthesis maps, may have denied the human race an opportunity to observe the 17th century Cas A supernova event itself.

Subject headings: interstellar: matter — interstellar: molecules — nebulae: supernova remnants

I. INTRODUCTION

The line of sight to the supernova remnant Cassiopeia A is characterized by a wealth of observational detail which offers an unusual opportunity to study physical and chemical conditions in the interstellar medium. Absorption lines detected in the spectrum of Cas A include those of H I, OH, H_2CO, NH_3, HCN, HCO^+, HC_5N, and HC_7N. These lines occur at velocities near 0 km s^{-1} (Local Arm gas) and at velocities between about −30 and −50 km s^{-1} (Perseus Arm gas). (See, for example, Encrenaz *et al.* 1980; Linke, Stark, and Frerking 1981; Bell, Feldman, and Matthews 1981; Batrla, Walmsley, and Wilson 1984, as well as references cited below.) The absorption of H I, OH, and H_2CO has been studied by aperture synthesis techniques: H I, Greisen (1973) and Kalberla, Schwarz, and Goss (1985); OH, Bieging and Crutcher (1985); H_2CO, Goss, Kalberla, and Dickel (1984). Moreover, a low-frequency (26.1 MHz) absorption line has been reported by Konovalenko and Sodin (1980) and identified by Blake, Crutcher, and Watson (1980) as a C II recombination line having n = 630. Emission lines of CH and CO have also been previously reported in the direction of Cas A by Rydbeck *et al.* (1976) and by Wilson *et al.* (1974) respectively.

Magnetic fields of 10 and 20 μG are known to exist in the Perseus Arm H I absorbing regions owing to detection of the Zeeman effect (Verschuur 1974). Yet the magnetic field in the Local Arm H I absorbing region is very small, less than 0.8 μG (Troland and Heiles 1982). Recently, the Perseus Arm magnetic field has been studied by Zeeman effect aperture synthesis techniques (Bregman *et al.* 1983; Schwarz *et al.* 1985), revealing a pattern of small-scale variations in field strength not readily detectable elsewhere in the interstellar medium.

Although CO lines have previously been detected toward Cas A (Wilson *et al.* 1974) and mapped (Scoville *et al.* 1977), a comprehensive study of the CO molecular emission has yet to be published. In this report we present ^{12}CO and ^{13}CO (J = 1–0) and ^{12}CO (J = 2–1) observations across the face of Cas A and at some adjacent positions. We derive from these data the distribution of the CO-emitting gas and its relationship to the distributions of other interstellar species, and we estimate physical conditions likely to exist within regions along the line of sight to Cas A.

II. OBSERVATIONS

We made the 115 GHz J = 1–0 ^{12}CO and 110 GHz J = 1–0 ^{13}CO observations with the NRAO 11 m telescope and cooled dual-polarization Cassegrain receiver.[1] The telescope half-power beam width (HPBW) is about 1.′1, and the velocity resolution is 0.26 and 0.65 km s^{-1}. We employed the absolute position-switched mode of operation, with the reference position located at 23^{h}26^{m}01.^{s}0, 56°38′47″ (1950), or 2° in galactic latitude south of the continuum source center. The spectral line intensities are expressed in terms of T_R^*, the source antenna temperature corrected for all relevant losses (Kutner and Ulich 1981). The radiation temperature T_R, required for computation of physical quantities in the line emitting regions, is related to

[1] The National Radio Astronomy Observatory is operated by Associated Universities, Inc., under contract to the NSF.

T_R^* by a beam efficiency factor n_c which we estimate to be 1.0 for a CO source with radius 4′ (see Ulich and Haas 1976).

For both ^{12}CO and ^{13}CO we observed a grid of 21 positions across the 4′ diameter face of Cas A, and for ^{12}CO only we observed selected positions due south and west of the source as much as 30′ away from source center. The grid spacing across Cas A itself is 1′ × 1′ in true angle on an equatorial coordinate system, with the center position (number 11) at $23^h21^m11^s.0$, 58°32′20″ (1950). (The grid positions are shown in Fig. 4, see § III.) In Figure 1 we present individual ^{12}CO and ^{13}CO spectra (Perseus Arm only) for a typical position (18) that is offset −2′ in right ascension and −1′ in declination from the source center. We also present in this figure an H I absorption spectrum for the same position derived from the synthesis data of Bregman *et al.* (1983).

We also mapped the $J = 1$–0 ^{12}CO emission in an extended area around Cas A with the Aerospace Corporation 4.6 m telescope operating in frequency-switching mode.[2] The Aerospace telescope has an HPBW of 2′.5 and a velocity resolution of 0.65 km s^{-1}. Within 3′ of the center of Cas A, we observed at spacings of 1′.5; outside this area the spacing of adjacent spectra is 3′ except at the very edges of the covered field where spacings are 6′. The area mapped extends 18′ to the north, east, and west of source center and 21′ to the south. Spectra obtained with the Aerospace telescope were scaled so that the line temperature observed in OMC-1 is the same as that observed with the NRAO telescope.

The peak-to-peak noise for all 0.65 km s^{-1} resolution ^{12}CO spectra (both Aerospace and NRAO telescopes) is about 1 K; the peak-to-peak noise for the corresponding ^{13}CO spectra (NRAO) is about 0.2 K. All velocities quoted here are with respect to the local standard of rest.

[2] The Aerospace Corporation millimeter wave telescope is operated by the Aerospace Corporation, Inc.

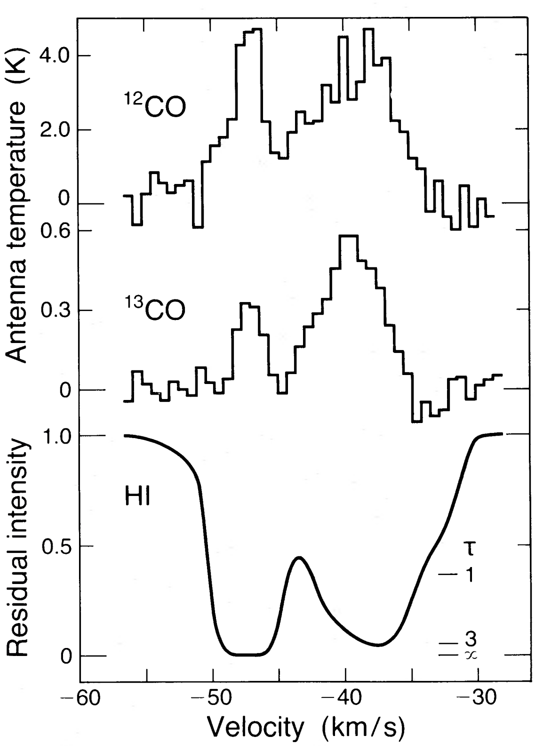

FIG. 1.—^{12}CO, ^{13}CO, and H I spectra for position 18 in front of Cas A. The spatial resolution of all three spectra is about 1′.1.

Finally, we observed the 231 GHz $J = 2$–1 ^{12}CO transition at three positions (11, 18, and 19) using the 4.9 m telescope of the Millimeter Wave Observatory.[3] This telescope has an HPBW of 1′.2 at the observing frequency, nearly the same as that of the NRAO 11 m telescope operating at 115 GHz. Therefore, comparisons between our $J = 2$–1 and $J = 1$–0 spectra of ^{12}CO are not complicated by significant beamwidth differences. All $J = 2$–1 spectra were calibrated by the chopper-wheel method, and they have been divided by an efficiency factor of 0.8 to convert to approximate radiation temperatures T_R.

For these observations, we position-switched the telescope to a reference position located at $23^h21^m10^s.9$, 58°32′44″ (1950). We obtained spectral information from two filter banks: one, with a velocity resolution of 1.3 km s^{-1}, covered both Local and Perseus Arm features; the other, with a velocity resolution of 0.33 km s^{-1}, covered the Local Arm only. Peak-to-peak noise in the lower resolution spectra is about 0.4 K.

III. SPATIAL STRUCTURE IN THE GAS

a) The Velocity Components

Interstellar gas toward Cas A with velocities near 0 km s^{-1} (Local Arm gas) probably lies within a few hundred parsecs of the Sun; gas at velocities of between about −30 and −50 km s^{-1} (Perseus Arm gas) is at a distance of order 3 kpc. High-sensitivity single-dish H I and OH absorption spectra of Cas A reveal a multitude of individual velocity components. Davies and Matthews (1972) have identified 11 such components, six of which are common to the spectra of both species. The Perseus Arm molecular gas is part of a large molecular complex that extends more than 4° along the galactic plane in the CO maps of Cohen *et al.* (1980), and also appears in the maps of Casoli, Combes, and Gerin (1984).

In Figure 2 we present the average 115 GHz ^{12}CO profile for all 21 on-source positions observed with the NRAO 11 m telescope. This source-averaged CO emission spectrum is not exactly equivalent to a single-dish absorption spectrum, because the latter is weighted by the continuum brightness temperature across the face of the source.

Several peaks appear in Figure 2, the most prominent of which are near velocities −1.5, −37.0, −40.6, and −47.2 km s^{-1}. Each of these velocities lies within about 0.5 km s^{-1} of a velocity component identified by Davies and Matthews in both the H I and OH spectra. Indeed, the source-averaged ^{12}CO spectrum possesses all velocity components identified in the single-dish OH absorption spectrum except for the most negative-velocity OH component at −48.8 km s^{-1}. Evidently, all CO-emitting molecular gas in the direction of Cas A is situated in front of the source, a circumstance that suggests Cas A lies on the far edge of the Perseus Arm. If the Perseus Arm is part of a trailing spiral density wave pattern, then the Cas A progenitor star was formed from material that entered the arm ahead of the atomic and molecular gas responsible for the Perseus Arm features of today.

The numerous velocity components visible in Figure 2 are not always identifiable in the individual spectra (especially in the ^{13}CO spectra) owing to sensitivity limitations. Therefore,

[3] The Millimeter Wave Observatory is operated by the Electrical Engineering Research Laboratory of the University of Texas at Austin, with support from the NSF, NASA, and McDonald Observatory.

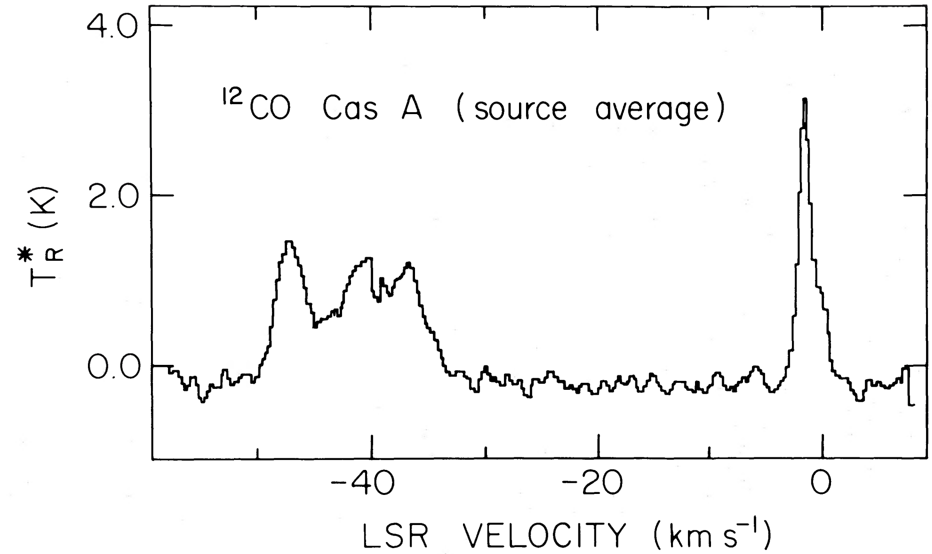

FIG. 2.—The average ^{12}CO spectrum across Cas A obtained by averaging spectra at 21 positions separated by 1.′1

for much of our analysis we consider just three principal CO "components": one close to -1.5 km s^{-1} (including all Local Arm gas), a second spanning the approximate range -35 to -44 km s^{-1}, and a third over the range -45 to -49 km s^{-1}. In Table 1 we present for each of these three components the peak $J = 1$–0 ^{12}CO and ^{13}CO line temperatures (T_R), as well as the ^{13}CO effective velocity widths. The latter are the ratios of the integrated line strengths (over the relevant velocity ranges) to the peak line temperatures.

b) Perseus Arm Gas between −35 and −44 km s^{-1}

The H I and OH gas between -35 and -44 km s^{-1} has two principal velocity components, centered at -37.6 and -41.1 km s^{-1} (Davies and Matthews 1972). The ^{12}CO spectra have components at similar velocities, and the strengths of these components show considerable spatial structure. In Figures 3*b* and 3*c* we present maps of the distribution of peak ^{12}CO line temperatures for these two components. The upper (circular) panels of each map show the on-source distribution derived from the NRAO telescope spectra; the lower panels represent peak ^{12}CO temperatures as observed by the Aerospace Corporation telescope. The small circles in the lower panels mark the approximate extent of Cas A, and they are equal in angular extent to the larger circular panels above.

Peak line temperatures near -37 and -40 km s^{-1} vary from less than 1 K to more than 4 K, with a local maximum in the distribution occurring several minutes west of Cas A. We detect no CO emission at all at most positions along the north rim of the source. The overall similarity in line temperature distribution for the two velocity components suggests that they are closely associated in space. Peak ^{13}CO line temperatures in the range -35 to -44 km s^{-1} are also greatest on the western

TABLE 1

PARAMETERS FOR CO LINES IN FRONT OF CASSIOPEIA A

	-1.5 km s^{-1}			-35 TO -44 km s^{-1}			-45 TO -49 km s^{-1}		
POSITION	T^{12}	T^{13}	ΔV	T^{12}	T^{13}	ΔV	T^{12}	T^{13}	ΔV
1...........	4.0	0.60	2.2	<1.0	<0.10	...	<0.7	<0.10	...
2...........	4.0	<0.15	...	<0.5	<0.10	...	<0.5	<0.15	...
3...........	4.2	0.35	1.4	<0.7	<0.15	...	<0.5	0.15	4.6
4...........	4.0	0.45	1.5	<0.8	<0.15	...	1.0	0.20	4.0
5...........	3.3	0.40	1.3	0.7	<0.15	...	0.8	<0.15	...
6...........	3.4	0.30	1.4	0.5	0.20	7.5	<0.5	0.12	4.8
7...........	4.5	0.25	1.5	1.5	0.15	6.7	1.3	0.10	3.8
8...........	3.0	0.25	2.2	2.0	0.50	6.5	0.5	<0.15	...
9...........	3.5	0.35	1.4	1.0	<0.15	...	2.0	<0.15	...
10...........	3.3	0.50	1.2	1.4	0.70	3.4	2.0	0.25	2.8
11...........	4.0	0.50	1.7	2.6	0.35	6.0	1.1	0.35	2.6
12...........	2.6	0.50	2.0	3.0	0.60	6.8	2.0	0.25	3.6
13...........	3.3	0.30	2.1	3.4	1.10	5.5	1.8	0.20	5.2
14...........	2.8	0.35	2.9	2.5	0.35	5.3	4.0	0.45	3.5
15...........	3.0	0.30	2.8	1.5	0.15	6.5	3.8	0.60	3.9
16...........	2.6	0.25	1.8	2.0	0.30	4.1	1.2	0.55	3.4
17...........	3.6	0.25	1.6	3.5	0.25	7.2	4.5	0.25	4.0
18...........	3.0	0.40	2.3	4.2	0.65	6.0	5.0	0.35	3.1
19...........	2.2	0.20	1.8	2.5	0.30	3.8	4.6	1.10	2.6
20...........	2.3	0.30	2.2	2.2	0.20	4.2	3.4	1.10	2.8
21...........	3.0	0.50	1.6	2.0	0.20	7.6	2.6	0.75	2.9

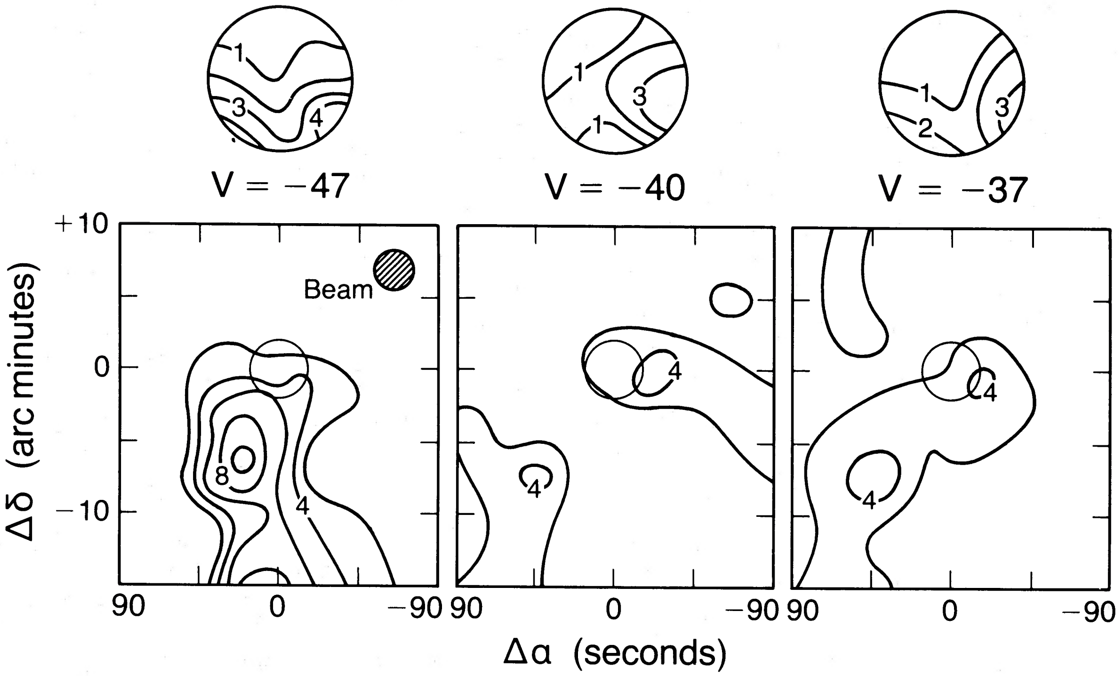

FIG. 3.—Maps of ^{12}CO peak line strength across the face of Cas A and at adjacent positions. The upper (circular) panels represent the line strengths in front of the source at 1'.1 resolution. The lower panels have a resolution of 2'.5, and the circles in these panels have the same angular diameter as those in the upper panels.

edge of the source, where they reach slightly more than 1 K. The $^{12}CO/^{13}CO$ line strength ratios are generally smaller than for the Local Arm gas, ranging from 2 to 14.

From the data of Table 1 we have computed excitation temperatures, ^{13}CO optical depths, and ^{13}CO column densities, using the standard procedure described by Dickman (1978) and by Blitz and Thaddeus (1980). That is, we assume the ^{12}CO line is optically thick and the excitation temperatures of the ^{12}CO and ^{13}CO species are equal. We derive CO excitation temperatures of between 3.5 and 7 K across the source, and ^{13}CO optical depths of 0.1–0.7. (Such low computed excitation temperatures are probably not reliable; most likely they are an artifact of clumping in the gas.) The distribution of $N(^{13}CO)$ is shown in Figure 4*b*. Considerable spatial structure is apparent, with the largest column densities occurring at the western edge of the source at a point nearly coincident with a strong peak in the Cas A continuum temperature (e.g., Bell 1977). Molecular hydrogen column densities inferred from these data lie in the range $0.3–2.5 \times 10^{21}$ cm^{-2} at those positions where both ^{12}CO and ^{13}CO have been detected. These values are up to 10 times higher than corresponding column densities in the Local Arm gas.

The distribution of $N(^{13}CO)$ in Figure 4*b* mimics very closely the distribution of H_2CO and OH optical depths across Cas A derived from aperture synthesis observations. Goss, Kalberla, and Dickel (1984) present 6 cm H_2CO optical depth maps with 10" resolution. These maps reveal the presence of numerous small-scale (10"–30" diameter) clumps of H_2CO spread along an east-west ridge across Cas A, with the greatest optical depths (above 1.0) occurring at the extreme western edge of the source. Figure 4*b* reveals a pattern that is similar in virtually all respects. The higher resolution OH synthesis maps of Bieging and Crutcher (1985) correspond very closely to the H_2CO maps. We conclude that the distributions of CO–, OH–, and H_2CO–bearing gas are all very similar, at least when averaged over angular scales of about 1'.

H I along the Cas A line of sight also shows enhanced column densities on the western side of the source. This effect is quite apparent in the earlier aperture synthesis maps of Greisen (1973), as well as in the more recent higher resolution (30") maps of Kalberla, Schwarz, and Goss (1985). For the purposes of direct comparison, we have integrated the Kalberla *et al.* H I profiles over the velocity range −33 to −43 km s^{-1}, after averaging adjacent profiles over 1' squared areas. H I column densities peak on the western side of the source, reaching values as high as 3.8×10^{21} cm^{-2}. However, the ratio of maximum to minimum column densities across Cas A is less than two for the atomic gas, compared to about five for the molecular (CO) gas. This difference is consistent with the expectation that the molecular gas exists within clumps that are embedded within larger regions of H I.

c) Perseus Arm Gas between −45 and −49 km s^{-1}

Gas at this velocity may have recently passed through a spiral density wave shock (Roberts 1972), with the densities thereby enhanced. The H I gas near this velocity has the highest optical depths of any in the Cas A spectrum, exceeding 4 or 5 over much of the source (Greisen 1973; Kalberla, Schwarz, and Goss 1985). Corresponding H I column densities usually exceed 3.0×10^{21} cm^{-2} and sometimes exceed 3.5×10^{21} cm^{-2}. Nonetheless, parameters of the CO gas near −47 km s^{-1} are not notably different from those at less negative velocities.

In Figure 3*a* we present the distribution of peak ^{12}CO line temperatures for the component centered near −47 km s^{-1}. Considerable spatial structure is apparent acrross the face of the source. No detectable emission exists along the north rim of Cas A, and a peak in line temperature lies about 7′ southeast of the source center. Peak temperatures for the ^{13}CO line are 3–20 times smaller than those for ^{12}CO.

From the data of Table 1 we derive CO excitation temperatures and ^{13}CO optical depths within the -45 to -49 km s^{-1} range with the same assumptions as for the less-negative-velocity Perseus Arm component (§ III*b*). In Figure 4*c* we present the distribution of $N(^{13}\mathrm{CO})$ across Cas A. These column densities are greatest at the southern and southeastern edge of the source. Molecular hydrogen column densities inferred from these data range from about 0.4 to 1.2×10^{21} cm^{-2} for positions with detected ^{12}CO and ^{13}CO emission. These values are about two times smaller than $N(H_2)$ inferred for the gas at -35 to -44 km s^{-1}. Since the minimum H I column densities for gas near -47 km s^{-1} are equal to or greater than the H I column densities at less negative Perseus Arm velocities, we conclude that the gas near -47 km s^{-1} has a smaller ratio of H_2 to H I than the gas in the velocity range -35 to -44 km s^{-1}.

For the gas near velocity -47 km s^{-1}, we find an excellent correspondence between the distribution of $N(^{13}\mathrm{CO})$, inferred from the present study, and the distribution of H_2CO revealed in the synthesis maps of Goss, Kalberla, and Dickel (1984).

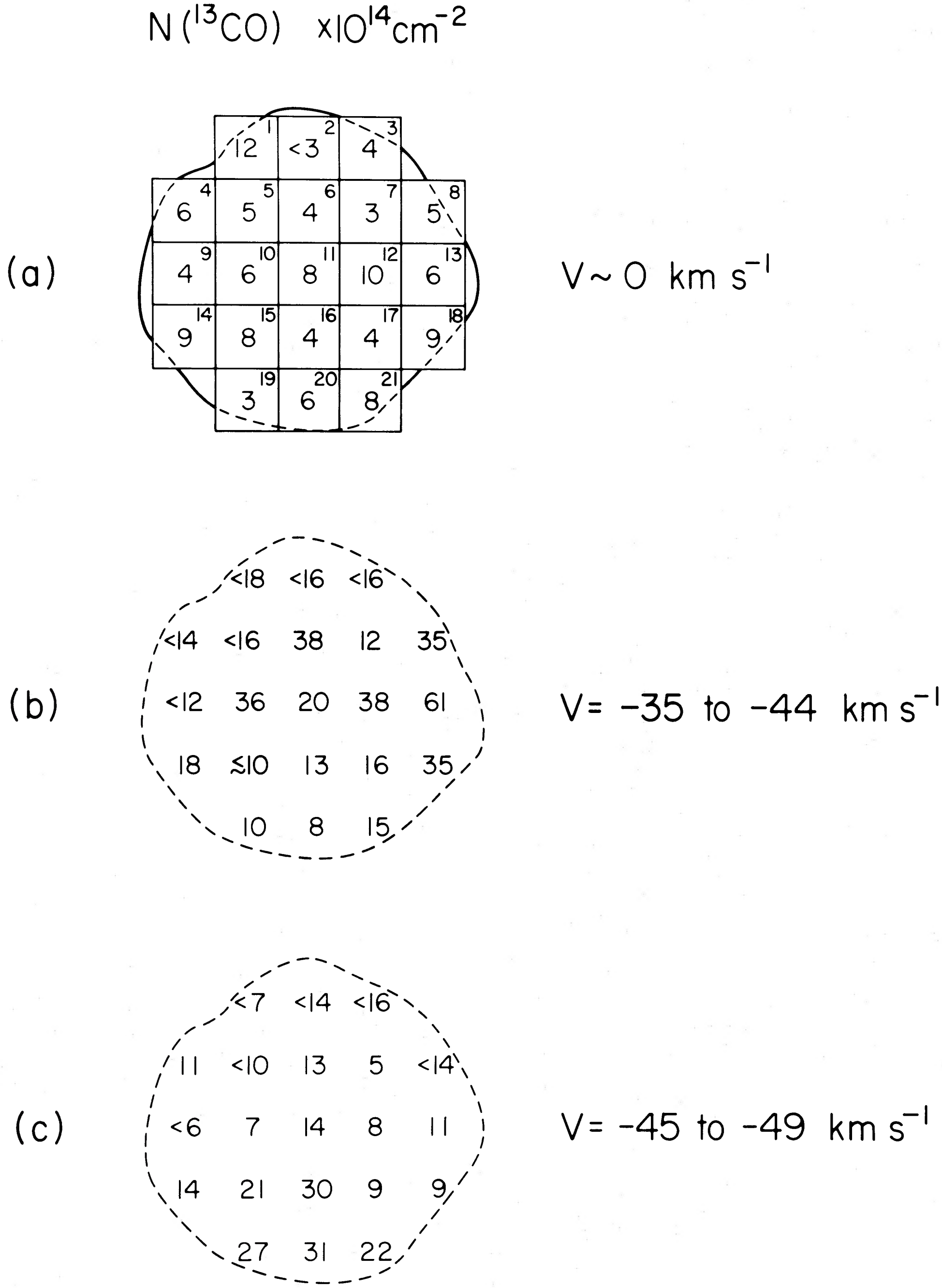

FIG. 4.—Maps of $N(^{13}\mathrm{CO})$ in front of Cas A at three velocities. These values have been derived under standard LTE assumptions (§ III*b*). The numbered boxes in Fig. 4*a* correspond to the position numbers in the first column of Table 1.

Small scale clumps of H_2CO having moderate optical depths (up to 0.3) lie along the southern and southeastern edge of Cas A, precisely those regions where $N(^{13}CO)$ is highest. The OH synthesis maps of Bieging and Crutcher (1985) reveal a comparable pattern of optical depths. No meaningful comparison between atomic and molecular gas distributions is possible at this velocity, owing to the H I line saturation.

d) The Local Arm Gas

The single-dish OH and H_2CO absorption spectra for the Local Arm reveal two well-separated components centered at about -0.1 and -1.5 km s^{-1} (e.g., Troland and Heiles 1974). The same two components appear in the H I spectrum, where they are highly blended. They also appear in our CO spectra; however, the one at -0.1 km s^{-1} is quite weak everywhere—usually about 1 K, or 2–3 times weaker than the component at -1.5 km s^{-1}.

Peak ^{12}CO line temperatures at -1.5 km s^{-1} show a small north-south gradient, varying from around 4 K at the north edge of the source to 2.5 K at the south, and reaching 2 K at a location 8′ south of the source center. Peak ^{13}CO line temperatures are 6–20 times smaller, and they show no obvious gradient.

Computing line parameters in the same manner as for the Perseus Arm gas, we derive CO excitation temperatures of between 6 and 7 K and ^{13}CO optical depths in the range 0.1–0.2 at various positions across the source.

In Figure 4*a* we present the distribution of ^{13}CO column densities $N(^{13}CO)$ across the face of Cas A. These values encompass both the Local Arm velocity components. No obvious pattern of spatial structure is apparent. CO column densities are uniform to within the limits of measurement error except for the high value in the northeast corner of the source. The ^{13}CO column densities can be converted to H_2 column densities $N(H_2)$ by assuming a ratio $N(^{13}CO)/N(H_2)$. Here we adopt the value 2×10^{-6} derived by Dickman (1978) from observations of thin dark clouds. In this case, $N(H_2)$ lies between 0.1 and 0.4×10^{21} for all Local Arm gas. The corresponding range of reddening $E(B-V)$ is 0.03–0.14 mag (Bohlin, Savage, and Drake 1978).

De Jager *et al.* (1978) have mapped the 6 cm H_2CO absorption in front of Cas A with 2′.6 resolution. They find that the stronger Local Arm feature (-1.5 km s^{-1}) increases in optical depth by about two times across the source, with the highest values occurring at the northeast edge of the source. H I column densities, estimated from the maps of Kalberla, Schwarz, and Goss (1985), are quite constant across the source with N(H I) about 1.3×10^{21} cm^{-2}. Here, and throughout this paper, we have assumed an excitation temperature of 80 K for the 21 cm transition.

IV. THE PHYSICAL NATURE OF THE GAS

a) General Distribution of Molecular and Atomic Gas

Estimates of ^{13}CO column density reveal spatial structure on angular scales of 1′–2′ across the face of Cas A (Fig. 4). At a distance of 3 kpc, this structure is equivalent to linear scales of $\sim$1–2 pc. For both of the Perseus Arm components, the CO distribution corresponds quite closely with those of H_2CO and OH. Moreover, the Perseus Arm gas seen in front of Cas A is part of a larger distribution of molecular material that extends in our maps more than 10′ off-source and can be traced along the Galactic plane for at least 4°.

Note that the maps of CO emission near Cas A (Fig. 3) reveal no sign of disturbances associated with the supernova remnant itself. Nor is there any indication whatever in the ^{12}CO spectra of anomalously high- or low-velocity gas. (The low-resolution ^{12}CO spectra cover a velocity range of -105 to $+55$ km s^{-1}.) However, the absence of evidence for supernova-affected gas does not necessarily imply that the expanding remnant is remote from the molecular gas we observe. The supernova-driven blast wave should rapidly dissociate molecules it may encounter, rendering this material invisible in the CO maps.

The relationship between CO-bearing gas and H I is defined only at certain velocities by the present study. A general correlation does exist between spatial variations in CO and H I column densities over the velocity range -35 to -44 km s^{-1} (§ III*b*). At other velocities spatial correlations between CO and H I cannot be perceived—in the Local Arm little spatial structure is found for either species, and H I structure in the velocity range -45 to -49 km s^{-1} is masked by line saturation effects. Moreover, the present results cannot yield accurate estimates of the ratios of hydrogen nuclei in atomic form to those in molecular form because the H I excitation temperatures are not well known, because the H I line is saturated at some velocities, and because estimates made of the molecular gas column densities are probably too low (see below). However, if the H I excitation temperature is 80 K, and the calculated molecular column densities are approximately correct, then the ratio $N(\text{H I})/2N(H_2)$ is of order unity or slightly greater.

We suspect for several reasons that values of $N(H_2)$ inferred from the standard LTE analysis of CO lines are too low. Dickman (1978) finds from models of inhomogeneous isothermal collapsing clouds that underestimates of $N(^{13}CO)$ by more than a factor of 2 are possible if the visual extinction is 2 mag or less. Also, the ratio $N(^{13}CO)/A_v$ derived by Dickman (for extinctions greater than 1 mag) is greater by factors of 2–3 or more than the same ratio inferred from other studies. For example, Frerking, Langer, and Wilson (1982) find $N(^{13}CO)/A_v$ to be between 2 and 10 times lower than Dickman's value on the basis of a study of CO and visual extinction in the ρ Oph and Taurus molecular complexes. Young *et al.* (1982) derive similar results from a study of dark cloud B5. These ratios apply to visual extinctions from 1 to 3 or 4 mag, and in some cases more. We conclude that values for $N(H_2)$, inferred from the standard LTE procedure, could be underestimates by factors of 2, 3, or more.

b) Location of the Molecular Gas

The line of sight to Cas A must pass through many regions of the interstellar gas, including diffuse as well as dark clouds. Here we consider the environment in which the CO is likely to exist, and we argue that the CO resides in dark cloud–like regions having angular scales smaller than the 1′.1 beamwidth of the NRAO telescope.

For all velocity components, the ratio of ^{12}CO to ^{13}CO line temperatures is low enough to imply large optical depths in the ^{12}CO line. This ratio is as small as two at some positions, and values of five are common, particularly in the Perseus Arm features. Only if chemical fractionation effects are very effective can the requirement of high ^{12}CO optical depths be at least partially relieved. However, the most effective chemical fractionation, yielding enhancement ratios of as much as eight, requires very specific conditions of low temperature, moderate density (10^3 cm^{-3} or more), and visual extinctions of 2–3 mag (Langer 1977).

Large optical depths in the ^{12}CO lines, together with relatively small ^{12}CO line temperatures (2–4 K, see Table 1) ensure that the formally calculated excitation temperatures will be quite small, typically 6 K or less. These values are lower limits to the kinetic temperatures in the clouds. Yet, kinetic temperatures are unlikely to be so low. On theoretical grounds, kinetic temperatures are probably 10 K at the very least and 15 K or more in regions where the visual extinction is less than about 1.5 mag. (See Fig. 13 of Young *et al.* 1982.) Moreover, Batrla, Walmsley, and Wilson (1984) have detected the (1, 1) and (2, 2) inversion lines of NH_3 at selected positions in front of Cas A. From these observations they derive NH_3 rotational temperatures of about 20 K in Local and Perseus Arm gas, and they infer kinetic temperatures in the NH_3–bearing regions of about 20 K. We conclude that the ^{12}CO toward Cas A must be quite subthermally excited, or else the CO clouds are clumpy on an angular scale smaller than the beam width.

Contrary to the suggestions of Cernicharo, Guelin, and Bujarrabal (1984), we believe that very subthermal excitation of the CO is unlikely. Given a kinetic temperature of 15 K, a CO excitation temperature as low as 6 K is only expected if the gas density is very low, only a few hundred cm^{-3}. At such low densities, however, theoretical calculations of gas-phase chemistry predict that little carbon should be in the form of CO (Mitchell, Ginsberg, and Kuntz 1978). Also, values for $N(H_2)$ inferred for individual Perseus Arm line components are typically $1–2 \times 10^{21}$ cm^{-2}, with angular scales of variation of order 2′ or less (§§ III*b*, *c*). Therefore, low gas densities of a few hundred cm^{-3} would imply extensions of the emission regions along the line of sight significantly greater than their extensions in the plane of the sky, especially since the derived values of $N(H_2)$ are likely to be underestimates, as argued above. We conclude that a very significant subthermal excitation of the ^{12}CO lines is quite unlikely; instead, the CO–emitting gas must lie in clumps smaller than the 1′.1 beamwidth. The synthesis maps of H_2CO and OH absorption toward Cas A (§§ III*b*, *c*) reveal small-scale clumping of these species as well.

Clumping of the CO–emitting gas cannot be too extreme, however, since a very small beam filling factor would require unrealistically high CO excitation temperatures in the clumps in order to account for the observed ^{12}CO line temperatures. If the CO excitation temperature does not exceed 20 K, then the filling factor must be at least 0.2, comparable to that for OH and H_2CO. Higher angular resolution CO observations are needed to specify the detailed distribution of the CO–bearing gas and its relationship to regions of OH and H_2CO absorption.

In view of the relatively small ratios of ^{12}CO to ^{13}CO line temperatures, especially for the Perseus Arm components, the ^{12}CO (J = 1–0) lines are likely to have optical depths of order 5 or perhaps more. If so, the visual extinctions through the CO clumps should be at least 4 mag. Here we assume kinetic and excitation temperatures of 15 K, $N(H_2)/A_v = 10^{21}$ molecules cm^{-2} mag^{-1} (Bohlin, Savage, and Drake 1978), and $X(CO) = N(CO)/N(H_2) = 5 \times 10^{-5}$. (The latter ratio lies between 10^{-6}, appropriate for diffuse clouds, and $1–2 \times 10^{-4}$ for dark clouds. See, for example, Young *et al.* 1982.) Evidently, visual extinctions in the CO–bearing clumps are at least moderately high, and these regions more nearly resemble dark than diffuse clouds.

On other grounds we must also conclude that the CO along the line of sight to Cas A resides predominantly in dark cloud–like environments. For most positions across the face of the source, we estimate $N(^{13}CO)$ is about 4×10^{15} (all velocities); and for reasons given above (§ IV*a*), this figure is, if anything, an underestimate. The UV observations of CO made by Federman *et al.* (1980) indicate that in a *diffuse* cloud ($A_v < 1$) the ratio $N(^{13}CO)/A_v$ is about 10^{14}. Therefore, if the CO lies mostly in diffuse clouds like those studied by Federman *et al.*, then the visual extinction in front of Cas A must be at least 40. A 10 times higher ratio $N(^{13}CO)/A_v$, appropriate to dark clouds, resolves this dilemma.

c) Gas Densities

The existence of moderate-strength CO lines toward Cas A implies that molecular densities along this line of sight exceed a few hundred cm^{-3}. Moreover, we estimate that the presence of HCO^+ in absorption (rather than in emission) places upper limits on the gas density of between 10^4 and 10^5 cm^{-3}. The smaller of these limits applies if the lines are optically thick such that excitation is increased by radiation trapping. The larger limit arises from an assumption of small optical depth.

Recently, Batrla, Walmsley, and Wilson (1984) have derived molecular gas densities of 4×10^3 and 10^4 cm^{-3} for gas near -40 and -47 km s^{-1} respectively. These values come from a comparison of 6 and 2 cm H_2CO lines, and they are based on excitation models which assume that the two lines arise in the same volumes of gas. This assumption might not be correct, as discussed by Vanden Bout, Snell, and Wilson (1983). Goss, Kalberla, and Dickel (1984) have estimated gas densities more directly in the H_2CO clumps revealed by their synthesis maps. These values are in the range $0.5–2 \times 10^4$ cm^{-3}. However, Heiles and Stevens (1985) question the ratio of H_2CO to H_2 chosen by these authors, arguing that the densities may be 5 times smaller.

Finally, Cernicharo, Guelin, and Bajarrabal (1984) present several arguments suggesting that molecular gas densities toward Cas A are quite low, less than 10^3 cm^{-3}. Their reasoning is based on an application of large velocity gradient (LVG) formalism to the observed ratio of ^{12}CO J = 2–1 to J = 1–0 line strengths (see below), and upon excitation arguments involving the presence of HCO^+ lines in absorption (see above). We doubt that the CO and HCO^+ data warrant placing such stringent upper limits. The upper limits of Cernicharo *et al.* most likely result from their assumption of a rather high kinetic temperature ($T_k > 30$ K) and from the (not necessarily warranted) assumption of high optical depth in the HCO^+ lines.

We have estimated molecular gas densities in two ways. First, we use the hydrogen column densities inferred from the CO spectra. If the gas is clumpy on a scale smaller than the beamwidth, then the true column densities have been reduced by the beam filling factor to the apparent (i.e., computed) column densities, and an estimate of the gas density follows from the expression

$$n(H_2) = N(H_2)/(lf) .$$

Here, $N(H_2)$ is the column density computed from the LTE estimates of $N(^{13}CO)$, l is the scale size of the molecular clump, and f is the beam filling factor. For gas in the Perseus Arm, we find that $N(H_2) = 10^{21}$ cm^{-2} for a typical individual velocity component. Taking l = 1 pc and f = 0.2, we find $n(H_2)$ is about 2×10^3 cm^{-3}.

We have also estimated molecular gas densities from a comparison of line strengths in the $J = 2$–1 and $J = 1$–0 lines of ^{12}CO observed at positions 11, 18, and 19 in front of Cas A. This procedure makes use of the large velocity gradient (LVG) radiative transfer models of Goldsmith, Young, and Langer (1983). Unfortunately, line saturation and other effects render these estimates uncertain, as discussed below.

In the absence of line saturation, the line temperature ratio T_{2-1}/T_{1-0} is a direct measure of $n(H_2)$, since the former increases monotonically with the latter in a way that depends on the kinetic temperature (see Figs. 3–12 of Goldsmith, Young, and Langer 1983). Moreover, values of the line ratio which deviate appreciably from unity (i.e., $T_{2-1}/T_{1-0} < 0.5$ or > 1.2) can arise only when the lines are not saturated. The *low* line ratios are characteristic of densities of order 10^3 cm^{-3} or less, while the high ratios signify densities of about 5×10^3 cm^{-3} or more. Note that clumping of the gas on a scale smaller than the telescope beamwidth will not affect the observed line ratios as long as beamwidths for the $J = 2$–1 and $J = 1$–0 transitions are comparable. In our measurements, this criterion is met (§ II).

A major concern in applying LVG models to our ^{12}CO data is the possibility of heavy line saturation. Indeed, saturation of these lines is assumed in the standard procedure we have used to estimate gas column densities (§ III). However, line saturation in the LVG models is mitigated by systematic velocity gradients in the emission regions which restrict the volume of space within which a photon can be trapped. No evidence exists in our CO spectra for velocity gradients across the face of Cas A. Even so, large velocity gradients could conceivably exist in the CO–emitting regions if the gas motions responsible for the line widths of individual line components arise in small clumps of gas. In short, ^{12}CO line saturation is not inevitable in these regions, and for several positions in front of the source we have observed line temperature ratios T_{2-1}/T_{1-0} significantly different from the unity value expected in the case of full line saturation.

The Local Arm component is so narrow that it is not fully resolved in the 1 MHz (1.3 km s^{-1}) resolution spectra of the $J = 2$–1 line. For one position (18), we did obtain a higher resolution (250 kHz) spectrum. However, the ratio T_{2-1}/T_{1-0} at this position is 0.8, not significantly different from the value of unity expected for saturated lines. Thus, no density estimate is possible.

For the Perseus Arm components, the ratios T_{2-1}/T_{1-0} are all less than one, in some cases significantly so. For example, gas in the velocity range -35 to -44 km s^{-1} is characterized by ratios of 0.5–0.7, implying gas densities of 1–2×10^3 cm^{-3} or less. Line ratios near -47 km s^{-1} are about 0.3 at positions 18 and 19. No LVG solution exists for these ratios at any temperature, because such small ratios imply very subthermal excitation, which is insufficient to account for the observed line temperatures. Such apparently nonphysical ratios T_{2-1}/T_{1-0} can arise if the 2–1 and 1–0 transitions do not originate in the same regions, as a result, for example, of the effects of the different optical depths in the two transitions. (Direct radiative excitation of the transitions by the Cas A supernova itself is ruled out by the weakness of the continuum radiation even if the gas is in close proximity to the remnant.)

In summary, the available evidence concerning gas densities in the Cas A CO–emitting clouds suggests values in the range 10^3–10^4 cm^{-3}. In the Perseus Arm components, for which small-scale spatial variations are revealed by our data, and for which the ratio T_{2-1}/T_{1-0} is small, gas densities most likely lie at the lower end of this range, perhaps a few times 10^3 cm^{-3}. These values are comparable to those inferred by Heiles and Stevens (1985) from the H_2CO synthesis data of Goss, Kalberla, and Dickel (1984).

d) Optical Extinction to Cas A

Optical images of Cas A reveal a system of small filaments and knots which are brightest along the northern and northeastern rim of the source (see, for example, Dickel *et al.* 1982; van den Bergh and Kamper 1983). Very deep plates emphasizing the [S II] lines at 6717 and 6713 Å reveal faint nebulosity extending around most of the rim of the source. However, no optical nebulosity whatever has been detected at the western edge of the rim, and few optical features lie within the central region of the source. Barring an extremely irregular distribution of optically luminous remnant material, the optical extinction in front of Cas A must be quite variable, with lowest extinctions occurring in the north and northeast and highest extinctions occurring in the west and possibly toward the central part of the source.

Early measurements of the visual extinction to Cas A relied on eye estimates of relative line strengths. On this basis Minkowski (1957) derived a (photographic) extinction of about 4 mag in the northern rim of the source. Shklovsky (1968) estimated that the extinction toward the source center was in excess of 6.5 mag; otherwise a Type II supernova with M_v of -16.5 should have been observed in the 17th century as at least a 4th magnitude object. Searle (1971) has performed the only photometric measurement yet reported, finding that $E(B - V) = 1.43$ mag in the direction of the bright 20″ long filament along the northeast rim of the source. Taking $R = 3.1$, this measurement implies a visual extinction of 4.4 mag along a line of sight that is certainly among the least heavily obscured to the source. Finally, van den Bergh (1971) reports $E(B-V) = 0.96$ mag for his star *a* located midway between our positions 12 and 13. Therefore, A_v is about 3.0 mag for this star which has an estimated distance of about 2 kpc and so must lie well in front of Cas A and, perhaps, in front of the Perseus Arm as well. These estimates of the visual extinction to Cas A are mostly comparable to or slightly lower than the statistically expected extinction of 5.7 mag along a 3 kpc path length in the Galactic plane (Spitzer 1978). However, the optically derived estimates of extinction are biased in favor of lines of sight having comparatively low extinction.

We now compare the optically derived visual extinctions with those inferred from molecular and atomic column densities toward Cas A. (The latter are derived from the H I synthesis maps of Kalberla, Schwarz, and Goss 1985, assuming $T_{ex} = 80$ K.) Here we also assume the standard ratio $N(H)/E(B-V) = 5.8 \times 10^{21}$ cm^{-2} mag^{-1} (Bohlin, Savage, and Drake 1978), where $N(H) = N(H\ I) + 2N(H_2)$. Note that visual extinctions derived from the radio data are averages over the 1′.1 beamwidth of the radio telescopes. Since the molecular gas is clumped on scales smaller than this, actual extinctions along particular lines of sight must be higher.

Searle's filament is closely coincident with our position 5, for which we detect CO in the Local but not in the Perseus Arm. At this position the radio data call for $A_v = 4.2$ mag if the Perseus Arm components are assumed to contain no molecular gas, and $A_v = 5.1$ mag if our upper limits to Perseus Arm molecular gas are included. These values are very close to the measured extinction of Searle; however, the agreement may be somewhat fortuitous. Unless our derived values for $N(H_2)$ are gross underestimates, most of the hydrogen nuclei along this particular line of sight are in atomic form; hence, our estimates of N(H) depend sensitively upon the value of T_{ex} assumed for the 21 cm transition. Nonetheless, the close correspondence between A_v derived from radio and optical measurements supports the idea that radio measurements of column densities are approximately correct.

We also compare the radio-estimated extinction toward van de Bergh's star *a* with his measured value of 3.0 mag. Column densities in the Local Arm account for an A_v of only 1 mag. This circumstance suggests that the star does not lie completely in front of the Perseus Arm, as van den Bergh suggests it might.

Encouraged by the correspondence at position 5 between radio and optically derived visual extinctions, we have estimated from the radio data the extinctions at each of the 21 CO positions in front of Cas A. These results are somewhat complicated by the fact that at some positions we have only upper limits on the molecular gas column densities (CO not detected), and at some positions we have only lower limits upon the atomic gas column densities (H I saturated at velocities near -47 km s^{-1}). The latter deficiency is probably not too important because upper limits to the H I column density at this velocity usually account for only about 25% of the total N(H). Therefore, N(H) cannot be too strongly influenced by undetected H I near -47 km s^{-1} unless actual H I optical depths are of order twice the upper limits of about 5 in the Kalberla *et al.* maps.

With these limitations in mind, we estimate from the radio data that visual extinctions (averaged over a 1.'1 beamwidth) do not vary by more than about 3 or 4 mag across the face of Cas A. Most of the extinction evidently arises within the rather uniformly distributed atomic gas; spatial structure in the extinction comes primarily from clumpiness in the molecular gas, particularly that in the Perseus Arm. The Local Arm gas is quite uniformly distributed across the source, accounting for about 1 mag of extinction. Radio-derived extinctions are lowest along the north and northeast rim, with values of 4–5 mag typical. Across the remainder of Cas A, A_v is at least 5–6 mag, except at the western edge of the source (position 13), for which A_v exceeds 8 mag. We quote lower limits for these latter positions because of saturation in the H I absorption lines near -47 km s^{-1} for all but the northeast sector of the source. The high extinction at position 13 is no doubt largely an effect of the marked concentration of molecular gas revealed in the H_2CO synthesis maps of Goss, Kalberla, and Dickel (1984). Note that van den Bergh's (1971) bright star *B* coincides quite closely with our position 13 and with an exceptionally bright knot of radio and X-ray emission. Fabian *et al.* (1980) speculate that this star might somehow be responsible for the knot; however, this is almost certainly not the case. From data provided by van den Bergh (1971), we estimate that A_v is about 1.2 for the star, rendering it a foreground object.

The general pattern of extinction inferred from the radio data is consistent with inferences that can be drawn from a comparison between the optical nebulosity and the brightness distribution of 0.1–4 keV X-rays presented by Murray *et al.* (1979) and by Fabian *et al.* (1980). Murray *et al.* point out that the X-ray map seems to correspond more closely to the distribution of optical knots emitting strongly in the S II lines than to any other optical tracers of the supernova remnant. This correspondence is most striking when the X-ray map is compared to the map of S II–emitting knots and faint nebulosity presented by Kamper and van den Bergh (1976). The shaded regions of faint nebulosity mimic very closely the outlines of X-ray emission for all regions of the source rim except the western edge. Even the faint jet of optical filaments issuing from the northeast sector of the source is reproduced quite clearly in the X-ray map. We suspect, on this empirical basis, that the X-ray map provides a good general guide to the run of unobscured optical nebulosity. If so, then comparison of the X-ray map with the optical filaments yields an independent picture of the distribution of optical obscuration. On this basis all general features of the extinction distribution across Cas A which we have inferred from the radio data are reproduced, particularly the low extinctions to the north and northeast and the unusually high extinction on the western side of the source.

Finally, we consider the question of why the Cas A supernova itself was not reported by contemporary (17th century) observers. The progenitor is believed to have been a massive star ($M > 9\ M_\odot$, Lamb 1978), and the supernova itself was presumably an unusual event since it gave rise to a very radio-luminous remnant; one which, as Minkowski (1968) has noted, would still be among the six strongest nonthermal radio sources in the sky if it were located anywhere in the Galaxy. If the absolute visual magnitude of the supernova was -17, and the distance is 3 kpc, then the apparent visual magnitude would have been -4.6 in the absence of extinction. Assuming (after Shklovsky 1968) that the object would have been noticed had its true apparent magnitude been 4 or less, then the extinction to the star must have been 8.6 mag or more. The (beam-averaged) extinction for our center position 11 is 5.7 mag. If the contribution from H I near -47 km s^{-1} is as much as double our lower limit for this position, then the estimated extinction is 7.3 mag. We are still left with a small (and possibly insignificant) discrepancy.

This discrepancy, however, may be resolved by the H_2CO synthesis maps of Goss, Kalberla, and Dickel (1984). Of the 16 small molecular gas concentrations they identify in front of the source, one (their number IX) is centered only 7″ away from the center of the explosion as derived by van den Bergh and Kamper (1983). This cloud has a full-width at half maximum of 20″ and an H_2 column density through its center of 2.2×10^{21} cm^{-2} (assuming the ratio of H_2CO to H_2 suggested by Heiles and Stevens 1985). If the line of sight to the supernova intersects 60% of this column density, then the cloud accounts for an extinction of at least 1.5 mag over and above the 7 mag or so contributed by more diffuse gas (see above). The chance alignment of a small knot of molecular gas directly in front of the progenitor star may have deprived the human race of an opportunity to witness one of the rarest phenomena in the recorded history of the cosmos.

This research was supported in part by an NSF grant to Carl Heiles.

REFERENCES

Batrla, W., Walmsley, C. M., and Wilson, T. L. 1984, *Astr. Ap.*, **136**, 127.
Bell, A. R. 1977, *M.N.R.A.S.*, **179**, 573.
Bell, M. B., Feldman, P. A., and Matthews, H. E. 1981, *Astr. Ap.*, **101**, L13.
Bieging, J. H., and Crutcher, R. M. 1985, in preparation.
Blake, D. H., Crutcher, R. M., and Watson, W. D. 1980, *Nature*, **287**, 707.
Blitz, L., and Thaddeus, P. 1980, *Ap. J.*, **241**, 676.
Bohlin, R. C., Savage, B. D., and Drake, J. F. 1978, *Ap. J.*, **224**, 132.
Bregman, J. D., Troland, T. H., Forster, J. R., Schwarz, U. J., Goss, W. M., and Heiles, C. 1983, *Astr. Ap.*, **118**, 157.
Casoli, F., Combes, F., and Gerin, M. 1984, *Astr. Ap.*, **133**, 99.

Cernicharo, J., Guelin, M., and Bajarrabal, V. 1984, preprint.
Cohen, R. S., Cong, H., Dame, T. M., and Thaddeus, P. 1980, *Ap. J.* (*Letters*), **239**, L53.
Davies, R. D., and Matthews, H. E. 1972, *M.N.R.A.S.*, **156**, 253.
de Jager, G., Graham, D. A., Wielebinski, R. S., Booth, R. S., and Gruber, G. M. 1978, *Astr. Ap.*, **64**, 17.
Dickel, J. R., Murray, S. S., Morris, J., and Wells, D. C. 1982, *Ap. J.*, **257**, 145.
Dickman, R. L. 1978, *Ap. J. Suppl.*, **37**, 407.
Encrenaz, P. J., Stark, A. A., Combes, F., Linke, R. A., Lucas, R., and Wilson, R. W. 1980, *Astr. Ap.*, **88**, L1.
Fabian, A. C., Willingale, R., Pye, J. P., Murray, S. S., and Fabbiano, G. 1980, *M.N.R.A.S.*, **193**, 175.
Federman, S. R., Glassgold, A. E., Jenkins, E. B., and Shaya, E. J. 1980, *Ap. J.*, **242**, 545.
Frerking, M. A., Langer, W. D., and Wilson, R. W. 1982, *Ap. J.*, **262**, 590.
Goldsmith, P. F., Young, J. S., and Langer, W. D. 1983, *Ap. J. Suppl.*, **51**, 203.
Goss, W. M., Kalberla, P. M. W., and Dickel, H. R. 1984, *Astr. Ap.*, **139**, 317.
Greisen, E. W. 1973, *Ap. J.*, **184**, 363.
Heiles, C., and Stevens, M. 1983, *Ap. J.*, submitted.
Kalberla, P. M. W., Schwarz, U. J., and Goss, W. M. 1985, in preparation.
Kamper, K., and van den Bergh, S. 1976, *Ap. J. Suppl.*, **32**, 351.
Konovalenko, A. A., and Sodin, L. G. 1980, *Nature*, **283**, 360.
Kutner, M. L., and Ulich, B. L. 1981, *Ap. J.*, **250**, 341.
Lamb, S. A. 1978, *Ap. J.*, **220**, 186.
Langer, W. D. 1977, *Ap. J.* (*Letters*), **212**, L39.
Linke, R. A., Stark, A. A., and Frerking, M. A. 1981, *Ap. J.*, **243**, 147.
Minkowski, R. 1957, in *IAU Symposium 4, Radio Astronomy*, ed. H. C. van de Hulst (Cambridge: Cambridge University Press), p. 107.
———. 1968, in *Stars and Stellar Systems*, Vol. 7, *Nebulae and Interstellar Matter*, ed. B. M. Middlehurst and L. H. Aller (Chicago: University of Chicago Press), p. 623.
Mitchell, G. F., Ginsburg, J. L., and Kuntz, P. J. 1978, *Ap. J. Suppl.*, **38**, 39.
Murray, S. S., Fabbiano, G., Fabian, A. C., Epstein, A., and Giacconi, R. 1979, *Ap. J.* (*Letters*), **234**, L69.
Roberts, W. W. 1972, *Ap. J.*, **173**, 259.
Rydbeck, O. E. H., Krollberg, E., Hjalmarson, A., Sume, A., Ellder, J., and Irvine, W. M. 1976, *Ap. J. Suppl.*, **31**, 333.
Schwarz, U. J., Troland, T. H., Albinson, J., Bregman, J. D., Goss, W. M., and Heiles, C. E. 1985, *Ap. J.*, submitted.
Scoville, N. Z., Irvine, W. M., Wannier, P. G., and Predmore, C. R. 1977, *Ap. J.*, **216**, 320.
Searle, L., 1971, *Ap. J.*, **168**, 41.
Shklovsky, I. S. 1968, *Supernovae* (London: Wiley), p. 90.
Spitzer, L. 1978, *Physical Processes in the Interstellar Medium* (New York: Wiley).
Troland, T. H., and Heiles, C. 1974, *Ap. J.*, **194**, 43.
———. 1982, *Ap. J.*, **252**, 179.
Ulich, B. L., and Haas, R. W., 1976, *Ap. J. Suppl.*, **30**, 247.
van den Bergh, S. 1971, *Ap. J.*, **165**, 259.
van den Bergh, S., and Kamper, K. W. 1983, *Ap. J.*, **268**, 129.
Vanden Bout, P. A., Snell, R. L., and Wilson, T. L. 1983, *Astr. Ap.*, **118**, 337.
Verschuur, G. L. 1974, in *Galactic and Extra-Galactic Radio Astronomy*, ed. G. L. Verschuur and K. I. Kellermann (New York: Springer-Verlag), p. 179.
Wilson, W. J., Schwartz, P. R., Epstein, E. E., Johnson, W. A., Etcheverry, R. D., Mori, T. T., Berry, G. G., and Dyson, H. B. 1974, *Ap. J.*, **191**, 357.
Young, J. S., Goldsmith, P. F., Langer, W. D., Wilson, R. W., and Carlson, E. R. 1982, *Ap. J.*, **261**, 513.

RICHARD M. CRUTCHER: Astronomy Department, 341 Astronomy Building, University of Illinois, Urbana, IL 61801

CARL HEILES: Astronomy Department, University of California, Berkeley, CA 94720

THOMAS H. TROLAND: Physics and Astronomy Department, University of Kentucky, Lexington, KY 40506